Gauge theories with overlap fermions in an arbitrary representation: Evaluation of the 3-loop β-function

M. Constantinou, H. Panagopoulos

Department of Physics, University of Cyprus,
P.O.Box 20537, Nicosia CY-1678, Cyprus
email: phpgmc1@ucy.ac.cy, haris@ucy.ac.cy

Abstract

This work presents the calculation of the relation between the bare coupling constant g_0 and the $\overline{\text{MS}}$-renormalized coupling $g_{\overline{\text{MS}}}$, $g_0 = Z_g(g_0, a\mu)g_{\overline{\text{MS}}}$, to 2 loops in perturbation theory, with fermions in an arbitrary representation of the gauge group $SU(N)$. Our calculation is performed using overlap fermions and Wilson gluons, and the background field technique has been chosen for convenience. The corresponding results in the fundamental representation appear in our longer publication [1].

The 3-loop coefficient of the bare β-function, b_2^L, is extracted using the 2-loop expression for Z_g, and it is presented as a function of the overlap parameter ρ, the number of fermion flavors (N_f) and the number of colors (N). We also provide the expression for the ratio $\Lambda_L/\Lambda_{\overline{\text{MS}}}$, in an arbitrary representation. A plot of $\Lambda_L/\Lambda_{\overline{\text{MS}}}$ is given in the adjoint representation.

Keywords: Beta function, Overlap fermions, Running coupling constant, Lattice perturbation theory.

PACS numbers: 11.15.Ha, 12.38.Gc, 12.38.Bx, 11.10.Gh.

I. INTRODUCTION

In this letter we present a computation of the bare β-function in the lattice formulation of the $SU(N)$ gauge theory, with N_f flavors of overlap fermions in an arbitrary representation of the gauge group $SU(N)$. This work is a sequel to a longer publication [1], in which the computation was performed with fermions in the fundamental representation. We will refer to [1] for the general background and notation.

While the main application of $SU(N)$ gauge theories on the lattice regards QCD, where fermions are in the fundamental representation of $SU(3)$, there has recently been some interest in gauge theories with fermions in other representations and with $N \neq 3$. Such theories are being studied in various contexts [2–9], e.g., supersymmetry, phase transitions, and the 'AdS/QCD' correspondence.

In later years, use of non-ultralocal actions which preserve chiral symmetry on the lattice has become more viable for numerical simulations. The two actions which are being used most frequently are overlap fermions [10–12] based on the Wilson fermion action and domain-wall fermions [13,14].

Overlap fermions are notoriously difficult to study, both numerically and analytically. Many recent promising investigations involving simulations with overlap fermions have appeared; see, e.g., Refs. [15–21]. Regarding analytical computations, the only ones performed thus far have been either up to 1 loop, such as Refs. [22–28], or vacuum diagrams at higher loops [29,30]. *The present work (along with Ref. [1]) is the first one involving non-vacuum diagrams beyond the 1-loop level.*

We compute the 2-loop renormalization Z_g of the bare lattice coupling constant g_0 in the presence of overlap fermions. We relate g_0 to the renormalized coupling constant $g_{\overline{\rm MS}}$ as defined in the $\overline{\rm MS}$ scheme at a scale $\bar{\mu}$; at large momenta, these quantities are related as follows

$$\alpha_{\overline{\rm MS}}(\bar{\mu}) = \alpha_0 + d_1(\bar{\mu}a)\alpha_0^2 + d_2(\bar{\mu}a)\alpha_0^3 + ...,\tag{1}$$

($\alpha_0 = g_0^2/4\pi$, $\alpha_{\overline{\rm MS}} = g_{\overline{\rm MS}}^2/4\pi$, a : lattice spacing). The 1-loop coefficient $d_1(\bar{\mu}a)$ has been known for a long time; several evaluations of $d_2(\bar{\mu}a)$ have also appeared in the past $\sim$10 years, either in the absence of fermions [31,32], or using the Wilson [33] or clover [34,35] fermionic actions. Knowledge of $d_2(\bar{\mu}a)$, together with the 3-loop $\overline{\rm MS}$-renormalized β-function [36], allows us to derive the 3-loop bare lattice β-function, which dictates the dependence of the lattice spacing on g_0. In particular, it provides a correction to the standard 2-loop asymptotic scaling formula which defines the renormalization group invariant scale Λ_L. Ongoing efforts to estimate the running coupling from the lattice [37–40] have relied on a mixture of perturbative and non-perturbative investigations. As a particular example, relating $\alpha_{\overline{\rm MS}}$ to $\alpha_{\rm SF}$ (SF: Schrödinger Functional scheme), entails an intermediate passage through the bare coupling α_0; the conversion from $\alpha_{\overline{\rm MS}}$ to α_0 is then carried out perturbatively.

The present study, being the first of its kind in calculating 2-loop diagrams with overlap vertices and external momentum dependence, had a number of obstacles to overcome. One first complication is the size of the algebraic form of the Feynman vertices; as an example, the vertex with 4 gluons and a fermion-antifermion pair contains $\sim$724,000 terms when expanded. Upon contraction these vertices lead to huge expressions (many millions of terms); this places severe requirements both on the necessary computer RAM and on the

efficiency of the computer algorithms which we must design to manipulate such expressions automatically. Numerical integration of Feynman diagrams over loop momentum variables is performed on a range of lattices, with finite size L, and subsequent extrapolation to $L \to \infty$. As it turns out, larger L are required for an accurate extrapolation in the present case, as compared to ultra-local actions. In addition, since the results depend nontrivially on the parameter ρ of the overlap action, numerical evaluation must be performed for a sufficiently wide set of values of ρ, with an almost proportionate increase in CPU time. Extreme choices of values for ρ ($\rho \gtrsim 0$, $\rho \lesssim 2$) show unstable numerical behaviour, which is attributable to the spurious poles of the fermion propagator for these choices; this forces us to even larger L. A consequence of all complications noted above is an extended use of CPU time: Our numerical integration codes, which ran on a 32-node cluster of dual CPU Pentium IV processors, required a total of ~ 50 years of CPU time.

The paper is organized as follows: The necessary theoretical background for the β-function, Z_g and $\Lambda_L/\Lambda_{\overline{\text{MS}}}$ is given in Section II. Section III describes briefly the overlap action and Section IV provides details on our computation and results for the fundamental representation. A generalization of the above results to an arbitrary representation is carried out in Section V. We employ the formulae of Section V to find numerical results for the 3-loop β-function and the ratio $\Lambda_L/\Lambda_{\overline{\text{MS}}}$. Results for the adjoint representation appear in Section VI.

II. THEORETICAL BACKGROUND

For the lattice regularization a bare β-function is defined as

$$\beta_L(g_0) = -a \frac{dg_0}{da}\bigg|_{g,\bar{\mu}} \tag{2}$$

where $\bar{\mu}$ is the renormalization scale and g (g_0) the renormalized (bare) coupling constant. It is well known that in the asymptotic limit for QCD ($g_0 \to 0$), one can write the expansion of the β-function in powers of g_0, that is

$$\beta_L(g_0) = -b_0 \, g_0^3 - b_1 \, g_0^5 - b_2^L \, g_0^7 - ... \tag{3}$$

The coefficients b_0, b_1 are universal, regularization independent constants (see Eqs. (41), (42)). On the contrary, b_i^L ($i \geq 2$) depends on the regulator; it must be determined perturbatively. In the present work we calculate the coefficient b_2^L using the overlap fermionic action and Wilson gluons.

$\beta_L(g_0)$ can be computed from the renormalization function Z_g, which is defined through $g_0 = Z_g^{L,\overline{\text{MS}}}(g_0, a\bar{\mu})g$, and relates the bare lattice coupling to the one renormalized in the $\overline{\text{MS}}$ scheme. Up to 2-loops, Z_g can be written in the form

$$(Z_g^{L,\overline{\text{MS}}}(g_0, a\bar{\mu}))^2 = 1 + g_0^2 \, (2b_0 \ln(a\bar{\mu}) + l_0) + g_0^4 \, (2b_1 \ln(a\bar{\mu}) + l_1) + O(g_0^6) \tag{4}$$

The quantities b_0, b_1 and l_0 have been known in the literature for quite some time [36,22]; b_0 and b_1 are the same as those of the renormalized β-function.

3

The constant l_0 is related to the ratio of the Λ parameters associated with the particular lattice regularization and the $\overline{\text{MS}}$ renormalization scheme

$$\Lambda_L/\Lambda_{\overline{\text{MS}}} \equiv e^{l_0/(2b_0)} \tag{5}$$

For overlap fermions in the fundamental representation the exact form of l_0 has been given in Ref. [22]. The value of l_0 for different representations is presented in Section V.

One can extract b_2^L from Z_g through

$$b_2^L = b_2 - b_1 l_0 + b_0 l_1 \tag{6}$$

where b_2 is the 3-loop coefficient of the renormalized β-function in the $\overline{\text{MS}}$ scheme [36]. Thus, the evaluation of b_2^L requires only the determination of the 2-loop quantity l_1.

The most convenient and economical way to proceed with calculating $Z_g(g_0, a\bar{\mu})$ is to use the background field technique [41–43], in which the following relation is valid

$$Z_A(g_0, a\bar{\mu})Z_g^2(g_0, a\bar{\mu}) = 1 \tag{7}$$

where Z_A, defined as: $A^\mu(x) = Z_A(g_0, a\bar{\mu})^{1/2}A_R^\mu(x)$ is the background field renormalization function (A^μ (A_R^μ): bare (renormalized) background field). In this framework, instead of $Z_g(g_0, a\bar{\mu})$, it suffices to compute $Z_A(g_0, a\bar{\mu})$, with no need to evaluate any 3-point functions. For this purpose, we consider the background field one-particle irreducible (1PI) 2-point function at momentum p, both in the continuum and on the lattice. In the notation of Ref. [31], the lattice 2-point function $\Gamma_L^{AA}(p)_{\mu\nu}^{ab}$ can be expressed in terms of the scalar function $\nu(p)$

$$\sum_\mu \Gamma_L^{AA}(p)_{\mu\mu}^{ab} = -\delta^{ab}3\hat{p}^2\left[1 - \nu(p)\right]/g_0^2, \qquad \nu(p) = g_0^2\nu^{(1)}(p) + g_0^4\nu^{(2)}(p) + ... \tag{8}$$

($\hat{p}_\mu = (2/a)\sin(ap_\mu/2)$). There follows

$$Z_A = \frac{1 - \nu_R(p, \bar{\mu}, g)}{1 - \nu(p, a, g_0)} \tag{9}$$

where ν_R (as well as ω_R below) is the continuum counterpart of ν (ω) (in dimensional regularization, $\overline{\text{MS}}$ subtraction). The gauge parameter λ must also be renormalized (up to 1 loop), in order to compare lattice and continuum results

$$\lambda = Z_Q\lambda_0, \qquad Z_Q = 1 + g_0^2 z_Q^{(1)} + ... \tag{10}$$

(Z_Q: renormalization function of the quantum field). The coefficient $z_Q^{(1)}$ is obtained from the quantum field 1PI 2-point function on the lattice ($\Gamma_L^{QQ}(p)_{\mu\nu}^{ab}$) through

$$\sum_\mu \Gamma_L^{QQ}(p)_{\mu\mu}^{ab} = -\delta^{ab}\hat{p}^2\left[3\left(1 - \omega(p)\right) + \lambda_0\right], \qquad \omega(p) = g_0^2\omega^{(1)}(p) + \mathcal{O}(g_0^4) \tag{11}$$

$$z_Q^{(1)} = \omega^{(1)}(p, a, g_0) - \omega_R^{(1)}(p, \bar{\mu}, g) \tag{12}$$

In terms of the perturbative expansions Eqs. (8), (11), Z_g^2 becomes

4

$$Z_g^2 = \left[1 + g_0^2 \left(\nu_R^{(1)} - \nu^{(1)} \right) + g_0^4 \left(\nu_R^{(2)} - \nu^{(2)} \right) + \lambda_0 \, g_0^4 \left(\omega^{(1)} - \omega_R^{(1)} \right) \frac{\partial \nu_R^{(1)}}{\partial \lambda} \right]_{\lambda = \lambda_0} \tag{13}$$

Since the quantities of interest are gauge invariant, we choose to work in the bare Feynman gauge, $\lambda_0 = 1$, for convenience. In order to compute Z_A we need the expressions for $\nu_R^{(1)}$, $\nu_R^{(2)}$, $z_Q^{(1)}$, $\nu^{(1)}$, $\nu^{(2)}$. The $\overline{\text{MS}}$ renormalized functions ν_R, ω_R, necessary for this calculation to 2 loops can be found in Refs. [31] ($N_f = 0$) and [33] (arbitrary N_f).

For the lattice quantities, the gluonic contributions ($N_f = 0$) have been presented in previous publications [31,32] (for the Wilson gauge action)

$$\omega^{(1)}(p, \lambda_0 = 1) = -\frac{5N}{48\pi^2} \ln (a^2 p^2) - \frac{1}{8N} + 0.137286278291 N \tag{14}$$

$$\nu^{(1)}(p, \lambda_0 = 1) = -\frac{11N}{48\pi^2} \ln (a^2 p^2) - \frac{1}{8N} + 0.217098494367 N \tag{15}$$

$$\nu^{(2)}(p, \lambda_0 = 1) = -\frac{N}{32\pi^4} \ln (a^2 p^2) + \frac{3}{128N^2} - 0.01654461954 + 0.0074438722 N^2 \tag{16}$$

The fermionic diagrams that contribute to $\nu^{(1)}$ (1-loop) and $\nu^{(2)}$ (2-loop) appear in Fig.1 and Fig.2 of Ref. [1], where $\nu^{(2)}$ was perturbatively calculated for the first time using overlap fermions and Wilson gluons. The fermion part of $\omega^{(1)}$ coincides with that of $\nu^{(1)}$. For overlap fermions, there are no diagrams with a mass counterterm, by virtue of the exact chiral symmetry of the overlap action.

III. OVERLAP ACTION

In recent years, overlap fermions are being used ever more extensively in numerical simulations, both in the quenched approximation and beyond. This fact, along with the desirable properties of the overlap action, was our motivation to calculate the β-function with this type of fermions. The important advantage of the overlap action is that it preserves chiral symmetry while avoiding fermion doubling. It is also $\mathcal{O}(a)$ improved. The main drawback of this action is that it is necessarily non-ultralocal; as a consequence, both numerical simulations and perturbative studies are extremely difficult and demanding (in terms of human, as well as computer time).

The overlap action is given by [11]

$$S_{\text{overlap}} = a^8 \sum_{n,m} \bar{\Psi}(n) \, D_N(n, m) \, \Psi(m) \tag{17}$$

where $D_N(n, m)$ is the overlap-Dirac operator

$$D_N(n, m) = \rho \left[\frac{\delta_{n,m}}{a^4} - \left(X \frac{1}{\sqrt{X^\dagger X}} \right)_{nm} \right], \qquad X = \frac{1}{a^4} \left(D_W - \rho \right) \tag{18}$$

and D_W is the Wilson-Dirac operator (with the Wilson parameter r set to 1)

$$D_{\text{W}} = \frac{1}{2} \left[\gamma_\mu \left(\nabla_\mu^* + \nabla_\mu \right) - a \nabla_\mu^* \nabla_\mu \right], \qquad \nabla_\mu \psi(x) = \frac{1}{a} \left[U(x, \mu) \psi(x + a\hat{\mu}) - \psi(x) \right] \tag{19}$$

5

The overlap parameter ρ is restricted by the condition $0 < \rho < 2$ to guarantee the correct pole structure of D_N. The coupling constant is included in the link variables, present in the definition of X, and one must study the perturbative expansion of D_N in powers of g_0. The expansion of X in momentum space reads

$$X(p',p) = \underbrace{\chi_0(p)(2\pi)^4\delta_P(p'-p)}_{tree-level} + \underbrace{X_1(p',p) + X_2(p',p)}_{1-loop} + \underbrace{X_3(p',p) + X_4(p',p)}_{2-loop} + O(g_0^5) \quad (20)$$

where χ_0 is the inverse fermion propagator and X_i are the vertices of the Wilson fermion action with i gluons (p (p'): fermion (antifermion) momentum). The construction of all overlap vertices relevant to the present 2-loop computation make use of χ_0 and $X_1 - X_4$; these quantities can be written in the compact form

$$\chi_0(p) = \frac{i}{a}\sum_\mu \gamma_\mu \sin(ap_\mu) + \frac{1}{a}\sum_\mu \left(1 - \cos(ap_\mu)\right) - \frac{\rho}{a}$$

$$X_1(p',p) = g_0 \int d^4k\delta(p'-p-k)\sum_\mu A_\mu(k)V_{1,\mu}\left(\frac{p'+p}{2}\right)$$

$$X_2(p',p) = \frac{g_0^2}{2}\int \frac{d^4k_1 d^4k_2}{(2\pi)^4}\delta(p'-p-k_1-k_2)\sum_\mu A_\mu(k_1)A_\mu(k_2)V_{2,\mu}\left(\frac{p'+p}{2}\right)$$

$$X_3(p',p) = \frac{g_0^3}{3!}\int \frac{d^4k_1 d^4k_2 d^4k_3}{(2\pi)^8}\delta(p'-p-\sum_{i=1}^3 k_i)\sum_\mu \prod_{i=1}^3 A_\mu(k_i)\left[-a^2V_{1,\mu}\left(\frac{p'+p}{2}\right)\right]$$

$$X_4(p',p) = \frac{g_0^4}{4!}\int \frac{d^4k_1 d^4k_2 d^4k_3 d^4k_4}{(2\pi)^{12}}\delta(p'-p-\sum_{i=1}^4 k_i)\sum_\mu \prod_{i=1}^4 A_\mu(k_i)\left[-a^2V_{2,\mu}\left(\frac{p'+p}{2}\right)\right] \quad (21)$$

where

$$V_{1,\mu}(p) = i\gamma_\mu \cos(ap_\mu) + \sin(ap_\mu), \quad V_{2,\mu}(p) = -i\gamma_\mu a \sin(ap_\mu) + a \cos(ap_\mu) \quad (22)$$

In Eqs. (21) A_μ represents a gluon field. The use of the background field technique implies that instead of the generic gluon fields, one must consider all possible combinations of background (A) and quantum (Q) fields, which are generated through the replacement

$$e^{iag_0 A_\mu(x)} \rightarrow e^{iag_0 Q_\mu(x)} \cdot e^{iaA_\mu(x)} \quad (23)$$

For example,

$$X_3(p',p) = X_3^{QQQ}(p',p) + X_3^{QQA}(p',p) + X_3^{QAA}(p',p) + X_3^{AAA}(p',p) \quad (24)$$

where X_3^{QQA} is given by

$$X_3^{QQA}(p',p) = \frac{g_0^2}{4}\int \frac{d^4k_1 d^4k_2 d^4k_3}{(2\pi)^8}\delta(p'-p-k_1-k_2-k_3) \times$$

$$\sum_\mu \left[-a^2V_{1,\mu}\left(\frac{p'+p}{2}\right)\left(Q_\mu(k_1)Q_\mu(k_2)A_\mu(k_3) + A_\mu(k_3)Q_\mu(k_2)Q_\mu(k_1)\right)\right.$$

$$\left. + iaV_{2,\mu}\left(\frac{p'+p}{2}\right)\left(Q_\mu(k_1)Q_\mu(k_2)A_\mu(k_3) - A_\mu(k_3)Q_\mu(k_2)Q_\mu(k_1)\right)\right] \quad (25)$$

6

and similarly for the remaining terms of Eq. (24).

At this point we can proceed with the perturbative expansion of D_N in powers of g_0. D_N can be written as

$$D_N(k_1, k_2) = D_0(k_1)\,(2\pi)^4\,\delta^4(k_1 - k_2) + \Sigma(k_1, k_2) \qquad (26)$$

where $D_0(k_1)$ is the inverse propagator for zero mass fermions. $\Sigma(k_1, k_2)$ contains all the vertices of the overlap action; these are made of one fermion-antifermion pair and an arbitrary number of gluons (up to 4 gluons for the needs of the present work). The much simpler case of vertices with up to 2 gluons (and no background) can be found in Ref. [44]. The expansion of $\Sigma(k_1, k_2)$ to order g_0^4 was carried out in Ref. [1] yielding, after laborious analytical manipulations, all necessary vertices for the present calculation. (An essential step is the expansion of $1/\sqrt{X^\dagger X}$ using complex analysis, which is presented in Appendix A of Ref. [1].)

Upon substituting the expression for X_i's in the overlap vertices, the latter become extremely lengthy and complicated. For instance, the vertex with Q-Q-A-Ψ-$\overline{\Psi}$ consists of 9,784 terms, while the vertex with Q-Q-A-A-Ψ-$\overline{\Psi}$ has 724,120 terms.

IV. RESULTS IN THE FUNDAMENTAL REPRESENTATION

For the algebra involving lattice quantities, we make use of our symbolic manipulation package in Mathematica, with the inclusion of the additional overlap vertices. After a number of simplifications (involving group generators, Dirac matrices, trigonometric identities), one must extract the p-dependence of the expression corresponding to each diagram (p: external momentum). Each diagram may in principle depend on p as follows:

$$\alpha_0 + \alpha_1\,p^2 + \alpha_2\,p^2\,\ln a^2\,p^2 + \alpha_3\,p^2\,(\ln a^2\,p^2)^2 + \alpha_4\,(\textstyle\sum_\mu p_\mu^4)/p^2 + \mathcal{O}(p^4, p^4\,\ln a^2\,p^2)$$

where the coefficients α_i are typically 2-loop integrals with no external momenta, which must be evaluated numerically. The required numerical integrations are performed by optimized Fortran programs which are generated by our Mathematica 'integrator' routine. Each integral is expressed as a sum over the discrete Brillouin zone of finite lattices, with varying size L, and evaluated for different values of the overlap parameter ρ. The average length of the expression for each diagram, after simplifications, is about 2-3 hundred thousand terms. Finally, we extrapolate the results to $L \to \infty$; this procedure introduces an inherent systematic error, which we can estimate quite accurately. Infrared divergent diagrams must be summed up before performing the extrapolation.

The resulting expressions for $\nu^{(1)}(p)$ and $\nu^{(2)}(p)$ (after addition of all diagrams) are

$$\nu^{(1)}(p) = \nu^{(1)}(p)\big|_{N_f=0} + N_f\left[k^{(1)} + \frac{2}{3}\frac{\ln a^2 p^2}{(4\pi)^2} + \mathcal{O}((ap)^2)\right] \qquad (27)$$

$$\nu^{(2)}(p) = \nu^{(2)}(p)\big|_{N_f=0} + N_f\left[\frac{c^{(1,-1)}}{N} + Nc^{(1,1)} + \frac{1}{16\pi^2}(3N - \frac{1}{N})\frac{\ln a^2 p^2}{(4\pi)^2} + \mathcal{O}((ap)^2)\right] \qquad (28)$$

Coefficients $k^{(1)}$, $c^{(1,1)}$ and $c^{(1,-1)}$ depend on the overlap parameter ρ. Their numerical results are tabulated in Tables 1 and 2 of Ref. [1], for different values of ρ ($0 < \rho < 2$).

Eqs. (27), (28) comply with a number of conditions coming from comparison with continuum results and usage of Ward Identities. Indeed: **a.** The total contribution to the gluon mass adds to zero, as expected. **b.** The coefficients of the non-Lorentz invariant terms $((\sum_\mu p_\mu^4)/p^2)$ cancel. **c.** The terms with double logarithms correspond to the continuum counterparts. This has been checked diagram by diagram. **d.** Terms with single logarithms add up to their expected value, which is independent of ρ (although the expressions per diagram are ρ-dependent).

In Fig. 1 we plot the 2-loop coefficients $c^{(1,-1)}$ and $(-c^{(1,1)})$ for different values of the overlap parameter. The extrapolation errors are visible for $\rho \leq 0.4$ and $\rho \geq 1.7$. A plot of the 1-loop coefficient $k^{(1)}$ versus ρ appears in Fig. 3 of Ref. [1]; its value lies in the interval $0.007 < k^{(1)} < 0.009$ for a wide range of ρ values, $0.7 < \rho < 1.6$, which encompasses completely the choices made for ρ in numerical simulations.
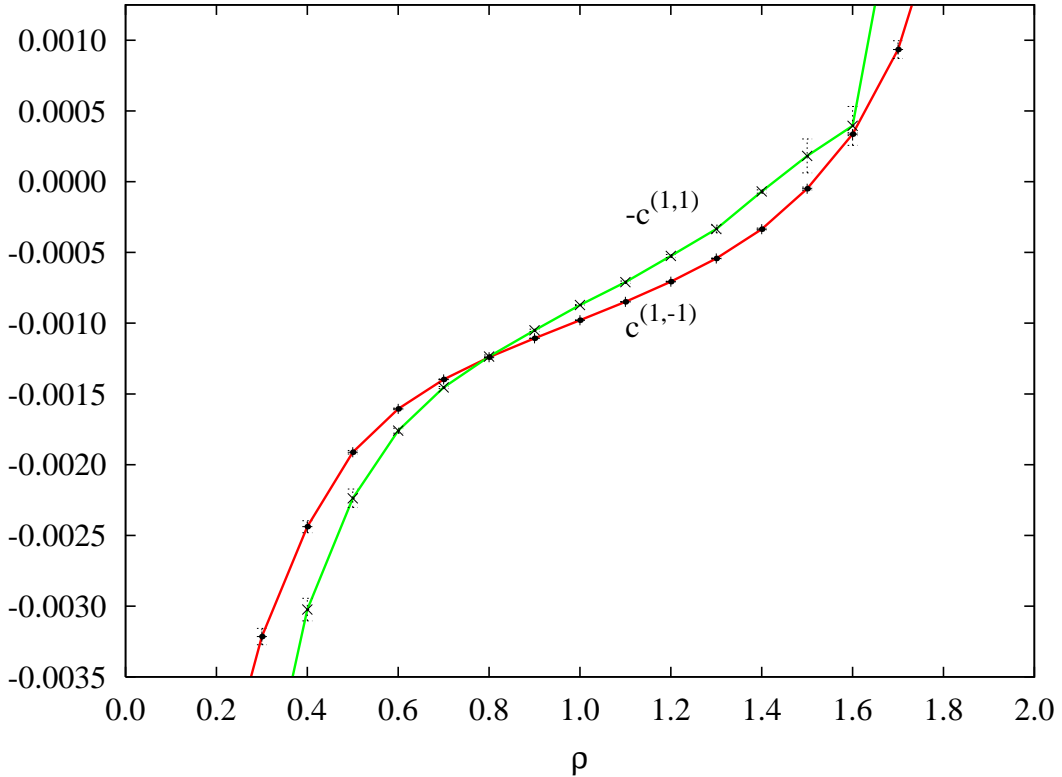

Fig. 1: Plot of the total 2-loop coefficients $c^{(1,-1)}$ and $(-c^{(1,1)})$ versus ρ.

Knowledge of the coefficients appearing in Eqs. (27), (28) allows us to derive l_0 (see Eq. (44) below) and l_1

$$l_1 = -\frac{3}{128\,N^2} + 0.018127763034 - 0.007910118514\,N^2$$

$$+N_f\left[\frac{1}{(16\pi^2)^2 N}\left(\frac{55}{12} - 4\zeta(3)\right) - \frac{N}{(16\pi^2)^2}\frac{481}{36} - \frac{N}{8\pi^2}k^{(1)} - \left(\frac{c^{(1,-1)}}{N} + Nc^{(1,1)}\right)\right] \qquad (29)$$

and therefore to find the 2-loop expression of Z_g. A direct outcome is the final form of the 3-loop coefficient b_2^L for the β-function (Eq. (6)), including gluonic as well as fermionic contributions; using Eqs. (41)-(44) and (29)

8

$$b_2^L = -\frac{11}{2048\pi^2\,N} + 0.000364106020\,N - 0.000092990690\,N^3$$

$$+N_f\left[\frac{(4\pi^2-1)^2}{4(16\pi^2)^3\,N^2} - 0.000046883436 - 000013419574\,N^2\right.$$

$$+\frac{N_f}{(16\pi^2)^3}\left(-\frac{23}{9\,N} + \frac{8\zeta(3)}{3\,N} + \frac{37\,N}{6}\right)$$

$$\left.-\frac{(11\,N - 2\,N_f)}{48\pi^2}\left(\frac{c^{(1,-1)}}{N} + c^{(1,1)}\,N\right) + \frac{(4\,N^3 + N_f - 3\,N^2\,N_f)}{(16\pi^2)^2\,N}k^{(1)}\right] \tag{30}$$

Eq. (30) is plotted against ρ for $N = 3$, $N_f = 0, 2, 3$ in Fig. 6 of Ref. [1]. In Section V we provide the equivalent expression for b_2^L in an arbitrary representation (Eq. (47)).

V. GENERALIZATION TO AN ARBITRARY REPRESENTATION

In this Section we provide the prescription that generalizes our results for $\nu^{(1)}$ and $\nu^{(2)}$ (Eqs. (27), (28)) to an arbitrary representation r, of dimensionality d_r. For the calculation under study, only the fermion part of the action is affected, with the link variables assuming the form

$$U_{x,\,x+\mu} = \exp(i\,g_0\,A_\mu^a(x)\,T_r^a) \tag{31}$$

where T_r^a denote the generators in the representation r, and satisfy the relations

$$[T_r^a, T_r^b] = i\,f^{abc}\,T_r^c, \quad \sum_a T_r^a T_r^a \equiv \mathbb{1}\,c_r, \quad \mathrm{tr}(T_r^a T_r^b) \equiv \delta^{ab}\,t_r = \delta^{ab}\,\frac{d_r\,c_r}{N^2-1} \tag{32}$$

In the fundamental representation F, one has

$$T_F^a \equiv T^a, \quad c_F = \frac{N^2-1}{2N}, \quad d_F = N, \quad t_F = \frac{1}{2} \tag{33}$$

Studying the color structures for each diagram with a fermionic loop reveals the appropriate substitutions one should make, in order to recast the results in an arbitrary representation. The generalization prescription can be summarized in what follows.

For the 1-loop contribution in the fundamental representation (Eq. (27)), the color structure is

$$\mathrm{tr}(T^a T^b) = \delta^{ab}\,t_F = \frac{1}{2}\,\delta^{ab} \tag{34}$$

Since diagrams with a closed fermion loop are always accompanied by a factor of N_f, the straightforward substitution

$$N_f \longrightarrow N_f \cdot (2\,t_r) \tag{35}$$

gives the desired results in an arbitrary representation.

9

For the 2-loop fermion contribution to $\nu^{(2)}$ (Eq. (28)), things get a bit more complicated, because there are different types of color structures. Fortunately, they all obey a general pattern, which will be given below. As an example, let us consider the following diagram, and describe step by step the extraction of the color dependence.
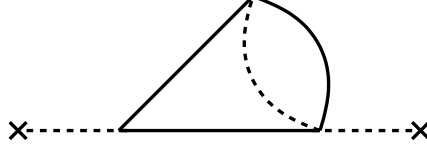

Fig. 2: A particular example of a 2-loop fermionic diagram. Dashed lines represent gluonic fields; those ending on a cross stand for background gluons. Solid lines represent fermions.

In all our diagrams, vertices with a fermion-antifermion pair and with 2 or more gluons contain also contributions involving integrations over internal momenta, and they are best depicted diagrammatically as non-pointlike vertices, as shown in Fig. 3.
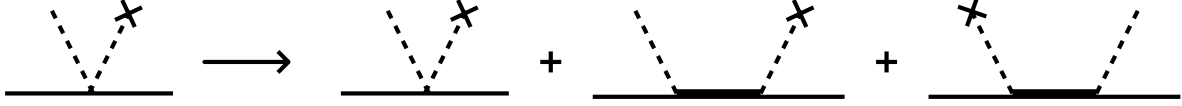

Fig. 3: The non-pointlike nature of an overlap vertex.

There is no propagator (and thus no poles) associated to the bold fermion lines. It is important to note that the color structures corresponding to such vertices are identical to those in ultra-local theories (with bold lines replaced by ordinary propagators). The diagram of Fig. 2 actually contains two subdiagrams (Fig. 4), arising from the non-pointlike contributions of the vertex of Fig. 3.
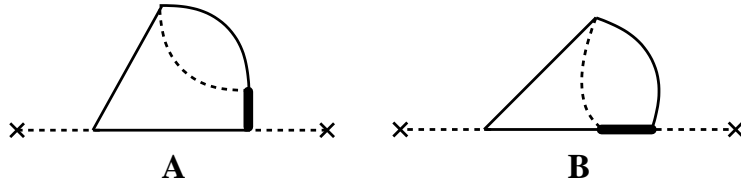

Fig. 4: The two parts of the diagram appearing in Fig. 2.

Subdiagram A has a color dependence of the type

$$\text{tr}(T^a T^c T^c T^b) = c_r \, t_r \, \delta^{ab} \tag{36}$$

(a, b color indices of the external lines), while subdiagram B has

$$\text{tr}(T^a T^c T^b T^c) = t_r \, \delta^{ab} \left(c_r - \frac{N}{2}\right) \tag{37}$$

10

Therefore, the color structure of the diagram in Fig. 2 has the form

$$\delta^{ab}\left(\alpha\, c_r\, t_r + \beta\, t_r\, (c_r - \frac{N}{2})\right) \tag{38}$$

In the fundamental representation, this expression becomes

$$\delta^{ab}\left(\alpha\, \frac{N^2 - 1}{4N} + \beta\,(-\frac{1}{4N})\right) \tag{39}$$

Thus, starting from our result for this diagram, which has the following color dependence: $(\alpha'N + \beta'/N)\,\delta^{ab}$, the prescription for converting it to another representation is

$$(\alpha'N + \beta'/N)\,\delta^{ab} = \left(4\alpha'\frac{N^2 - 1}{4N} - 4(\alpha' + \beta')(-\frac{1}{4N})\right)\,\delta^{ab}$$
$$\rightarrow \left(4\alpha'\, c_r\, t_r - 4(\alpha' + \beta')(c_r - \frac{N}{2})\, t_r\right)\,\delta^{ab} \tag{40}$$

One may check that all diagrams follow the formula above.

For the computation of b_2^L, we need also the expressions for b_0, b_1, b_2 in an arbitrary representation

$$b_0 = \frac{1}{(4\pi)^2}\left(\frac{11}{3}N - \frac{4}{3}t_r\, N_f\right) \tag{41}$$

$$b_1 = \frac{1}{(4\pi)^4}\left[\frac{34}{3}N^2 - t_r\, N_f\left(\frac{20}{3}N + 4c_r\right)\right] \tag{42}$$

$$b_2 = \frac{1}{(4\pi)^6}\left[\frac{2857}{54}N^3 + 2\,t_r\, N_f\left(c_r^2 - \frac{205}{18}c_r\, N - \frac{1415}{54}N^2\right) + 4\,t_r^2\, N_f^2\left(\frac{11}{9}c_r + \frac{79}{54}N\right)\right] \tag{43}$$

In order to calculate the ratio $\Lambda_L/\Lambda_{\overline{MS}}$, the quantity l_0 is necessary. For overlap fermions, it equals

$$l_0 = \frac{1}{8N} - 0.16995599N + 2\,t_r\, N_f\left[-\frac{5}{72\pi^2} - k^{(1)}\right] \tag{44}$$

Moreover, according to the prescriptions given in Eqs. (35), (40), the results for $\nu^{(1)}$ and $\nu^{(2)}$ become

$$\nu^{(1)}(p) = \nu^{(1)}(p)\Big|_{N_f=0} + 2\,t_r\, N_f\left[k^{(1)} + \frac{2}{3}\frac{\ln a^2 p^2}{(4\pi)^2} + \mathcal{O}((ap)^2)\right] \tag{45}$$

$$\nu^{(2)}(p) = \nu^{(2)}(p)\Big|_{N_f=0} + 4\,t_r\, N_f\left[c^{(1,1)}\frac{N}{2} - c^{(1,-1)}\left(c_r - \frac{N}{2}\right) + (c_r + N)\frac{\ln a^2 p^2}{(4\pi)^4} + \mathcal{O}((ap)^2)\right] \tag{46}$$

Finally, Eqs. (45), (46) lead to the 3-loop coefficient of the bare β-function, which in an arbitrary representation has the form

$$b_2^L = -\frac{11}{128\,(4\pi)^2}\frac{1}{N} + 0.000364106020\,N - 0.000092990690\,N^3$$

$$+ t_r\,N_f\left[\frac{1}{32\,(4\pi)^2}\frac{1}{N^2} + \frac{c_r}{2\,(4\pi)^4}\frac{1}{N} + \frac{2\,c_r^2}{(4\pi)^6} - 0.00011964262 - 0.00003220865\,c_r\,N\right.$$

$$- 0.00001086180\,N^2 + \frac{t_r\,N_f}{3\,(4\pi)^6}\left(\left(\frac{184}{3} - 64\,\zeta(3)\right)c_r + \left(\frac{130}{3} + 32\,\zeta(3)\right)N\right)$$

$$+ \frac{k^{(1)}}{32\,\pi^4}\left(-(c_r + N)\,t_r\,N_f + N^2\right) + \frac{c^{(1,-1)}}{24\,\pi^2}\,(2\,c_r - N)\,(-4\,t_r\,N_f + 11\,N)$$

$$\left.+ \frac{c^{(1,1)}}{24\,\pi^2}N\,(4\,t_r\,N_f - 11\,N)\right] \tag{47}$$

VI. ADJOINT REPRESENTATION

As a particular application, let us focus on the adjoint representation, A. The latter is encountered, e.g., in the standard supersymmetric extension of gauge theories in terms of vector superfields, where the gluinos are Majorana fermions in the adjoint representation, thus similar in many respects to $N_f = 1/2$ species of Dirac fermions.

The generators now take the form

$$(T_A^a)_{bc} \equiv i\,f_{bac} \tag{48}$$

and the dimensionality of A is $d_A = N^2 - 1$. Moreover,

$$c_A = N, \qquad t_A = \frac{d_A\,c_A}{N^2 - 1} = N \tag{49}$$

Eqs. (45) and (46) for $\nu^{(1)}$ and $\nu^{(2)}$ now read

$$\nu_{adj}^{(1)}(p) = \nu^{(1)}(p)\big|_{N_f=0} + N_f\,N\left[2\,k^{(1)} + \frac{4}{3}\frac{\ln a^2p^2}{(4\pi)^2} + \mathcal{O}((ap)^2)\right] \tag{50}$$

$$\nu_{adj}^{(2)}(p) = \nu^{(2)}(p)\big|_{N_f=0} + N_f\,N^2\left[2(c^{(1,1)} - c^{(1,-1)}) + \frac{\ln a^2p^2}{32\pi^4} + \mathcal{O}((ap)^2)\right] \tag{51}$$

It is interesting to find the numerical values of $\Lambda_L/\Lambda_{\overline{\text{MS}}}$ in the adjoint representation (its numerical values in the fundamental representation appear in Ref. [22]), which can be done using our 1-loop results for $k^{(1)}$. This ratio is defined through Eq. (5), where l_0 in this case is

$$l_0^{adj} = \frac{1}{8N} - 0.16995599N + 2\,N\,N_f\left[-\frac{5}{72\pi^2} - k^{(1)}\right] \tag{52}$$

Our results for $\Lambda_L/\Lambda_{\overline{\text{MS}}}$ are plotted in Fig. 5 for $N = 3$ and $N_f = 0, 1/2, 1$. One may compare Fig. 5 with an analogous figure pertaining to fermions in the fundamental representation (Ref. [22]); in that case, one obtains $0.02 \leq \Lambda_L/\Lambda_{\overline{\text{MS}}} \leq 0.025$, for $N_f = 1$.
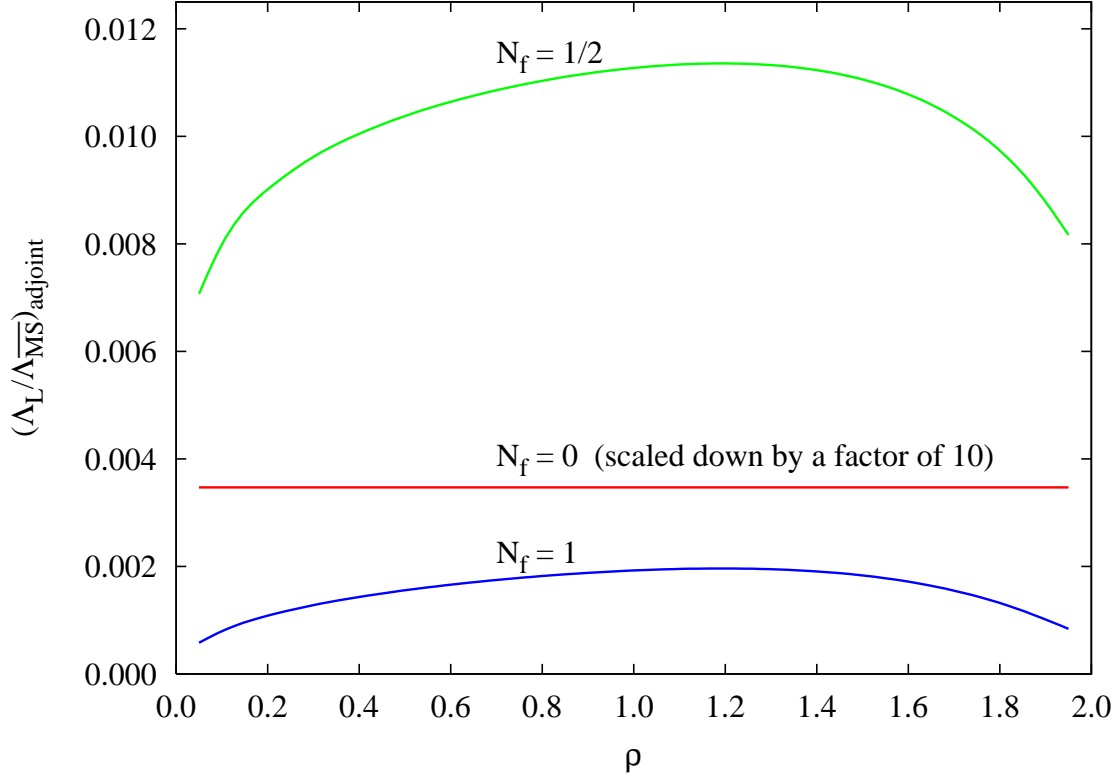
Fig. 5: The ρ dependence of the ratio $\Lambda_L/\Lambda_{\overline{\mathrm{MS}}}$ in the adjoint representation is plotted for $N = 3$ and $N_f = 0$ (horizontal line *scaled down by a factor of* 10 *from its value* 0.034711), $N_f = 1/2$ and $N_f = 1$.

13

REFERENCES

[1] M. Constantinou, H. Panagopoulos, Phys. Rev. **D**, to appear, [arXiv:0709.4368]

[2] P. Kovtun, M. Unsal, L. G. Yaffe, [hep-th/0702021]

[3] M. García Pérez, A. González-Arroyo, JHEP **0611** (2006) 091, [hep-th/0609058]

[4] G. Cossu at al., PoS(LAT2006)069, [hep-lat/0609049]

[5] S. Catterall, JHEP **0603** (2006), [hep-lat/0602004]

[6] F. Basile, A. Pelissetto, E. Vicari, PoS(LAT2005)199, [hep-lat/0509018]

[7] F. Sannino, Phys.Rev. **D72** (2005) 125006, [hep-th/0507251]

[8] A. González-Arroyo, R. Kirchner, JHEP **0601** (2006) 029, [hep-lat/0507036]

[9] J. Engels, S. Holtmann, T. Schulze, Nucl. Phys. **B724** (2005) 357, [hep-lat/0505008]

[10] R. Narayanan, H. Neuberger, Phys. Rev. Lett. **71** (1993) 3251, [hep-lat/9308011]

[11] H. Neuberger, Phys. Lett. **B417** (1998) 141, [hep-lat/9707022];
B427 (1998) 353, [hep-lat/9801031]

[12] H. Neuberger, Ann. Rev. Nucl. Part. Sci. **51** (2001) 23, [hep-lat/0101006]

[13] D.B. Kaplan, Phys. Lett. **B288** (1992) 342, [hep-lat/9206013]

[14] V. Furman, Y. Shamir, Nucl. Phys. **B439** (1995) 54, [hep-lat/9405004]

[15] T. DeGrand, Z. Liu, S. Schaefer, Phys. Rev. **D74** (2006) 099904, [hep-lat/0608019]

[16] T. Draper, N. Mathur, J. Zhang, A. Alexandru, Y. Chen, S.-J. Dong, I. Horvath, F.X. Lee, K.-F. Liu, S. Tamhankar, hep-lat/0609034

[17] O. Bär, K. Jansen, S. Schaefer, L. Scorzato, A. Shindler, PoS(LAT2006)199, [hep-lat/0609039]

[18] R. Babich, N. Garron, C. Hoelbling, J. Howard, L. Lellouch, C. Rebbi, hep-lat/0701023

[19] JLQCD collaboration: H. Fukaya et al., hep-lat/0702003

[20] J. Bloch, A. Frommer, B. Lang, T. Wettig, arXiv:0704.3486

[21] E.-M. Ilgenfritz, K. Koller, Y. Koma, G. Schierholz, T. Streuer, V. Weinberg, Phys. Rev. **D76** (2007) 034506, [arXiv:0705.0018]

[22] C. Alexandrou, H. Panagopoulos, E. Vicari, Nucl. Phys. **B571** (2000) 257, [hep-lat/9909158]

[23] C. Alexandrou, E Follana, H. Panagopoulos, E. Vicari, Nucl. Phys. **B580** (2000) 394, [hep-lat/0002010]

[24] S. Capitani, L. Giusti, Phys. Rev. **D62** (2000) 114506, [hep-lat/0007011]

[25] S. Capitani, Nucl. Phys. Proc. Suppl. **106** (2002) 826, [hep-lat/0108028]

[26] T. DeGrand, Phys. Rev. **D67** (2003) 014507, [hep-lat/0210028]

[27] M. Göckeler, R. Horsley, H. Perlt, P.E.L. Rakow, G. Schierholz, A. Schiller, PoS(LAT2006)161, [hep-lat/0610060]

[28] M. Ioannou, H. Panagopoulos, Phys. Rev. **D73** (2006) 054507, [hep-lat/0601020]

[29] A. Athenodorou, H. Panagopoulos, Phys. Rev. **D70** (2004) 077507, [hep-lat/0408020]

[30] A. Skouroupathis, H. Panagopoulos, Phys. Rev. **D72** (2005) 094509, [hep-lat/0509012]

[31] M. Lüscher, P. Weisz, Nucl. Phys. **B452** (1995) 234, [hep-lat/9505011]

[32] B. Allés, A. Feo, H. Panagopoulos, Nucl. Phys. **B491** (1997) 498, [hep-lat/9609025]

[33] C. Christou, A. Feo, H. Panagopoulos, E. Vicari, Nucl. Phys. **B525** (1998) 387, [hep-lat/9801007]

[34] A. Bode, H. Panagopoulos, Nucl. Phys. **B625** (2002) 198, [hep-lat/110211]

[35] A. Bode, H. Panagopoulos, Y. Proestos, Nucl. Phys. Proc. Suppl. **106** (2002) 832, [hep-lat/0110225]

[36] O.V. Tarasov, A.A. Vladimirov, A. Zharkov, Phys. Lett. **B93** (1980) 429

[37] R. Sommer, Lectures given at ILFTN Workshop on Perspectives in Lattice QCD, Nara, Japan, October 2005, [hep-lat/0611020]

[38] ALPHA Collaboration: M. Della Morte, R. Frezzotti, J. Heitger, J. Rolf, R. Sommer, U. Wolff, Nucl. Phys. **B713** (2005) 378, [hep-lat/0411025]

[39] O. Kaczmarek, F. Karsch, P. Petreczky, F. Zantow, Phys. Rev. **D70** (2004) 074505; Erratum-ibid. **D72** (2005) 059903, [hep-lat/0406036]

[40] Q. Mason, H.D. Trottier, C.T.H. Davies, K. Foley, A. Gray, G. P. Lepage, M. Nobes, J. Shigemitsu, Phys. Rev. Lett. **95** (2005) 052002, [hep-lat/0503005]

[41] L.F. Abbott, Nucl. Phys. **B185** (1981) 189

[42] R. K. Ellis, G. Martinelli, Nucl. Phys. **B235** (1984) 93

[43] M. Lüscher, P. Weisz, Nucl. Phys. **B452** (1995) 213, [hep-lat/9504006]

[44] Y. Kikukawa, A. Yamada, Nucl. Phys. **B547** (1999) 413, [hep-lat/9808026]